

# Scaling behavior of microwave reactors and discharge size for diamond deposition

T. Grotjohn<sup>a,\*</sup>, R. Liske<sup>b</sup>, K. Hassouni<sup>c</sup>, J. Asmussen<sup>a,b</sup>

<sup>a</sup>2120 Engineering Building, Electrical and Computer Engineering, Michigan State University, East Lansing, MI 48824, USA

<sup>b</sup>Fraunhofer Center for Coatings and Laser Applications, USA

<sup>c</sup>CNRS-LIMHP, France

Available online 18 January 2005

## Abstract

Several microwave reactors of various sizes were studied to quantify the size scaling behavior of microwave plasma-assisted CVD (PACVD) diamond deposition. All the systems studied were microwave resonant cavity based systems using predominantly hydrogen based discharges. The input variables considered include the microwave frequency (2.45 GHz and 915 MHz), the microwave power level, and the discharge chamber size (5–28 cm diameter). The substrate sizes for the various reactors studied ranged from 2.5 cm diameter substrates for the small reactor size to 15 cm diameter substrates for the large reactor size. The variables quantified in the diamond deposition process and reactor included the microwave discharge power density, discharge size, discharge gas temperature, as well as, measurements of diamond deposition area and rate. The discharge power density versus pressure and discharge size is quantified by experimental measurements and numerical modeling. Results show that as the discharge size increases the discharge power density decreases significantly at a given pressure.

© 2004 Published by Elsevier B.V.

*Keywords:* Diamond film; Simulation; Plasma CVD; Reactor modeling

## 1. Introduction

The scaling of microwave plasma-assisted CVD (PACVD) diamond deposition to larger area substrates has been done by several researchers by increasing the plasma discharge size [1–4]. This has been accomplished by scaling the microwave frequency from 2.45 GHz to 915 MHz and by increasing the microwave power going into the discharge. The performance of microwave plasma-assisted reactors as the discharge size increases from 3 cm diameter in a small reactor up to over 25 cm diameter in a large reactor can change substantially, especially considering the large increase in the ratio of discharge volume to discharge surface area as the size increases. This paper applies experimental measurements and computational models to quantify and understand

diamond PAVCD discharge and reactor size scaling properties and performance.

## 2. Experimental

Four diamond deposition reactor systems that range in plasma volume from 15 cm<sup>3</sup> to over 1000 cm<sup>3</sup> have been studied. Three of the systems (labeled A, C and D in Table 1) are based on a microwave cavity plasma reactor design [4–7] as shown in Fig. 1. The microwave discharge is produced inside a quartz dome that is located at one end of a microwave cavity. Microwave energy is transmitted from a microwave generator into the cavity using the coaxial excitation probe. In the reactors labeled A, C and D the substrate can be configured to be either thermally floating or actively cooled. In both configurations the substrate and substrate holder are heated by the plasma discharge. In the actively cooled configuration the

\* Corresponding author. Tel.: +1 517 353 8906; fax: +1 517 353 1980.

E-mail address: [grotjohn@egr.msu.edu](mailto:grotjohn@egr.msu.edu) (T. Grotjohn).

Table 1  
Sizes of the various reactor systems

Reactor name	Frequency (MHz)	Microwave cavity diameter (cm)	Quartz dome diameter (cm)	Substrate diameter (cm)	Plasma volume (cm <sup>3</sup> )
A	2450	17.8	5.1	2.5	15–30
B	2450	25	10	5	40
C	2450	17.8	12	7.5–10	100
D	915	60	28	15	1000

substrate holder is water cooled from below. In the thermally floating configuration the substrate holder sets on a quartz tube. The other system utilized is shown in Fig. 2 and is a bell jar system studied by Gicquel et al. [8]. The reactor is composed of a quartz bell jar surrounded by a 25 cm diameter Faraday cage that acts as a resonant cavity for the microwave fields. Each of the reactors studied has been demonstrated to deposit diamond of similar quality and linear growth rate as determined by the pressure and gas composition. The predominant gas composition utilized was hydrogen with a small percentage of methane (1 to few percent). In operation the larger diameter systems require more input microwave power to deposit diamond over larger substrate areas.

These reactors can be operated across a range of pressures from 10–140 Torr. An example range of operation of one of these reactor systems is shown in Fig. 3. This figure shows the substrate temperature for reactor C as a function of pressure and absorbed microwave power. The substrate temperature increases with the discharge operating pressure. Also, the discharge size increases as the microwave power increases and decreases as the pressure increases. The curve  $V_{dmin}$  indicates the minimum power at a given pressure necessary to have the plasma big enough in diameter to cover the substrate. The

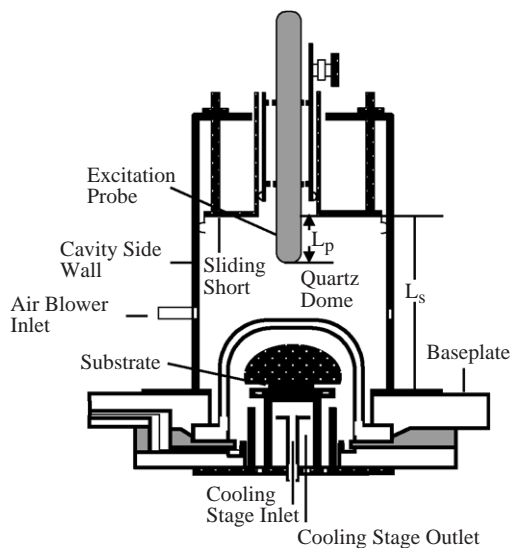


Fig. 1. Resonant cavity microwave reactor for diamond deposition. This figure is representative of reactors A, C, and D.

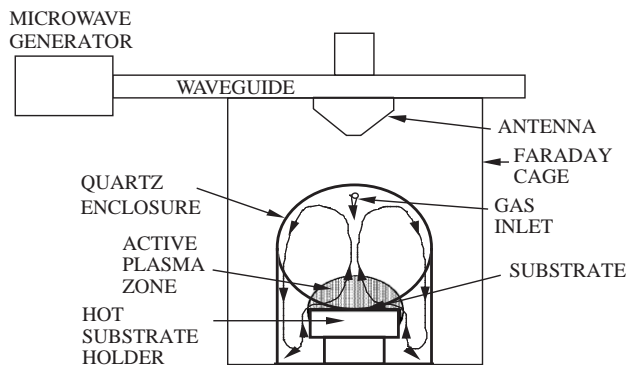


Fig. 2. Reactor B configuration.

curve  $V_{dmax}$  indicates the maximum power at a given pressure necessary to have the plasma just smaller in size than the quartz dome.

The plasma volume is defined as the region that has a high visual intensity. The plasma volume was determined at each pressure primarily by photographs taken through a window in the plasma reactor. The shape of the discharge is generally that of a sphere or hemisphere depending on the reactor system. For the reactor parameter range studied here, the diameter of the plasma near the substrate is set by adjusting the input microwave power so that the discharge diameter is approximately equal to the diameter of the substrate.

For the four reactor configurations the discharge power density was determined by dividing the absorbed microwave power by the discharge volume. The absorbed microwave power is the incident power minus the reflect power. Fig. 4 shows the discharge power density for the four systems for the pressure range from 10 to 85 Torr. For reactors A, C, and D the substrate holder was thermally floating. The power density is highest for the higher pressures and the smaller discharge size. For the largest reactor system (reactor D) the plasma discharge volume is approximately 1000 cm<sup>3</sup> and the power densities for the pressures studied are less than 10 W/cm<sup>3</sup>. At a given

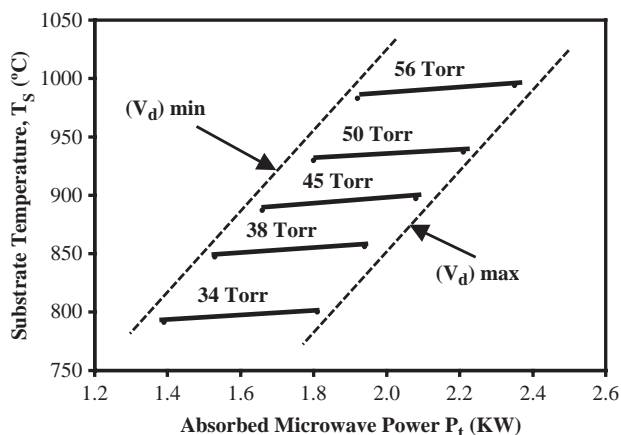


Fig. 3. Substrate temperature as a function of absorbed microwave power and pressure in reactor C with a thermally floating substrate holder.

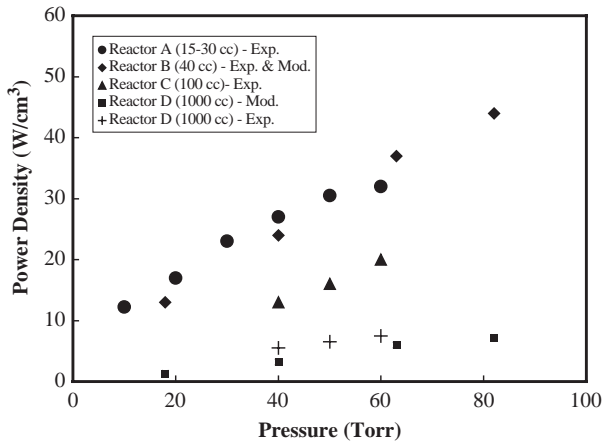


Fig. 4. Discharge power density versus pressure and discharge volume (in  $\text{cm}^3$ ).

pressure the scaling of the required microwave power versus substrate area is: microwave power  $\sim$  (substrate area) $^{0.75}$ . This scaling assumes that the discharge size is approximately hemispherical in shape.

### 3. Modeling and discussion

A microwave discharge reactor model [9] for hydrogen dominated discharges was used to numerically calculate the discharge behavior. This model was initially developed for reactor B and it has been verified by extensive experimental diagnostics as referenced and described in Ref. [9]. The agreement of the model with experimental data for Reactor B has been verified for the pressure range of 15–80 Torr for several parameters including discharge power density [9]; discharge gas temperature as measured by CARS [8], two-photon allowed LIF [10] and Doppler broadening optical emission spectroscopy [10]; and discharge atomic hydrogen dissociation fraction as measured by calibrated actinometry [11]. The power density data in Fig. 4 for reactor B indicates power density for both the model and experimental results. Because of the close agreement, only one symbol is used for each pressure condition.

This model was also applied to a large hydrogen discharge with a size of  $1000 \text{ cm}^3$ . This large discharge corresponds to reactor D and the model results for discharge power density are indicated in Fig. 4. The model results and experimental results for the power density are in close agreement. The experimental results for reactor D have an accuracy that is less than the other reactor systems because of the difficulty in viewing the discharge size through the available viewing ports. The accuracy is approximately 25%.

The model results not only include the power density but they also include the gas temperature, electron temperature and atomic hydrogen fraction as shown in Fig. 5. Fig. 5 includes the model results for both reactors B and D, i.e. 40 and  $1000 \text{ cm}^3$  discharges. The values shown in Fig. 5 are the

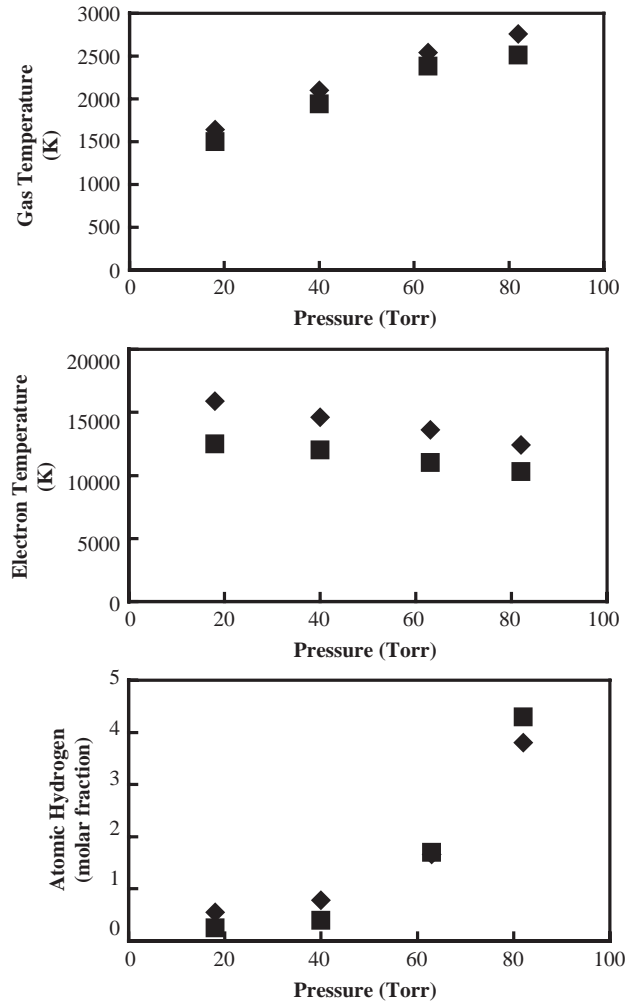


Fig. 5. Gas temperature, electron temperature and atomic hydrogen fraction versus pressure. Diamond shapes indicate reactor B and square shapes indicate reactor D.

average values in the plasma discharge region. The results show that the large discharge reactor as compared to the smaller reactor operates at a given pressure with a lower

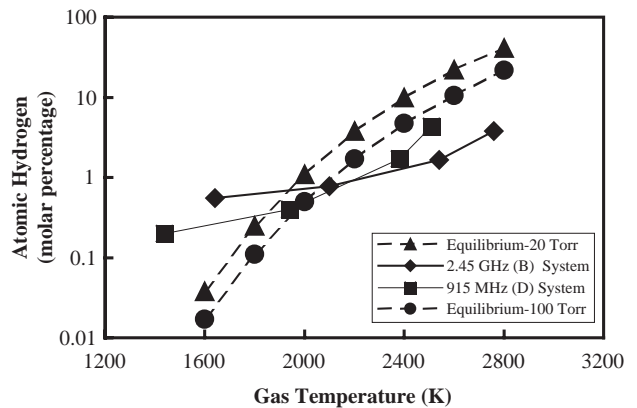


Fig. 6. Average atomic hydrogen molar fraction versus average gas temperature in the plasma discharge for reactors A and D operating with discharge sizes of 40 and  $1000 \text{ cm}^3$ , respectively. Also indicated is the equilibrium atomic hydrogen molar fraction versus gas temperature at 20 and 100 Torr.

discharge power density, a lower electron temperature, and a similar or just slightly lower gas temperature. The atomic hydrogen molar fraction behavior changes from lower for the larger discharge size as compared to smaller discharges at low pressures to higher for the larger discharge size at higher pressures. Additional understanding of the atomic hydrogen fraction behavior versus pressure is shown in Fig. 6. The data for gas temperature and atomic hydrogen fraction from Fig. 5 are plotted on the same graph. Also plotted on this graph is the equilibrium values for the atomic hydrogen fraction versus gas temperature from Argoitia et al. [12]. The equilibrium values would be those expected in an infinitely large discharge with no wall or surface losses. Fig. 6 shows that at low gas temperatures, which correspond to low pressures, the atomic hydrogen fraction is actually above that expected from equilibrium only considerations. This is explained by the atomic hydrogen dissociation occurring primarily by electron dissociation at the lower pressures of 40 Torr or less. Then as the pressure increases the atomic hydrogen molar fraction increases, especially as the gas temperature reaches 2400–2800 K. It can also be noted in Fig. 6 that the larger discharge has an atomic hydrogen molar fraction at the higher pressure (i.e. higher gas temperatures) that is closer to the equilibrium values than the smaller discharge. So at the pressure of 80 Torr in Fig. 5 the atomic hydrogen molar fraction is higher for the larger discharge even though the gas and electron temperatures are lower because the larger discharge is more equilibrium-like (i.e. a large volume plasma with minimal surface losses or gradients to surfaces) since the discharge volume to surface area is larger.

#### 4. Conclusion

For microwave plasma-assisted CVD of diamond the input power needed to create a plasma discharge large enough to cover a desired area does not scale linearly with discharge volume nor with substrate area. Rather the

required input power scales as (substrate area)<sup>0.75</sup>. Further, at higher pressures, above 50–60 Torr, the larger volume plasma as compared to smaller volume plasmas operate with higher fractions of atomic hydrogen because the discharge is closer to operating as a large-volume thermal equilibrium discharge with reduced plasma surface or wall losses. Both the scaling of the required input microwave power versus substrate size and the higher molar fractions of atomic hydrogen at high pressures above 50–60 Torr indicate that larger discharges operate more efficiently in terms of power density to maintain the plasma and in terms of atomic hydrogen dissociation percentage at a selected pressure.

#### References

- [1] S. Schelz, C. Campillo, M. Moisan, *Diamond and Related Materials* 7 (1998) 1675.
- [2] M. Funer, C. Wild, P. Koidl, *Applied Physics Letters* 72 (1998) 1149.
- [3] T. Tachibana, Y. Ando, A. Watanabe, Y. Nishibayashi, K. Kobashi, T. Hirao, K. Oura, *Diamond and Related Materials* 10 (2001) 1569.
- [4] T.A. Grotjohn, J. Asmussen, in: J. Asmussen, D.K. Reinhard (Eds.), *Diamond Films Handbook*, Dekker, New York, 2001.
- [5] J. Zhang, B. Huang, D.K. Reinhard, J. Asmussen, *Journal of Vacuum Science & Technology. A. Vacuum, Surfaces, and Films* 8 (1990) 2124.
- [6] K.-P. Kou, J. Asmussen, *Diamond and Related Materials* 6 (1997) 1097.
- [7] T.A. Grotjohn, J. Asmussen, J. Sivagnaname, D. Story, A.L. Vikharev, A. Gorbachev, A. Kolysko, *Diamond and Related Materials* 9 (2000) 322.
- [8] A. Gicquel, K. Hassouni, S. Farhat, Y. Breton, C.D. Scott, M. Lefebvre, M. Prelat, *Diamond and Related Materials* 3 (1994) 581.
- [9] K. Hassouni, T.A. Grotjohn, A. Gicquel, *Journal of Applied Physics* 86 (1999) 134.
- [10] A. Gicquel, M. Chenevier, Y. Breton, M. Petiau, J.P. Booth, K. Hassouni, *Journal de Physique. III* 6 (1996) 1167.
- [11] A. Gicquel, M. Chenevier, K. Hassouni, A. Tserepi, M. Dubus, *Journal of Applied Physics* 83 (1998) 7504.
- [12] A. Argoitia, et al., in: M. Prelas, G. Popovici, L.K. Bigelow (Eds.), *Handbook of Industrial Diamonds and Diamond Films*, Dekker, New York, 1998.